NASA Technical Memorandum 4362

Quasi-Elastic Nuclear Scattering at High Energies

Francis A. Cucinotta, Lawrence W. Townsend,
and John W. Wilson

MAY 1992

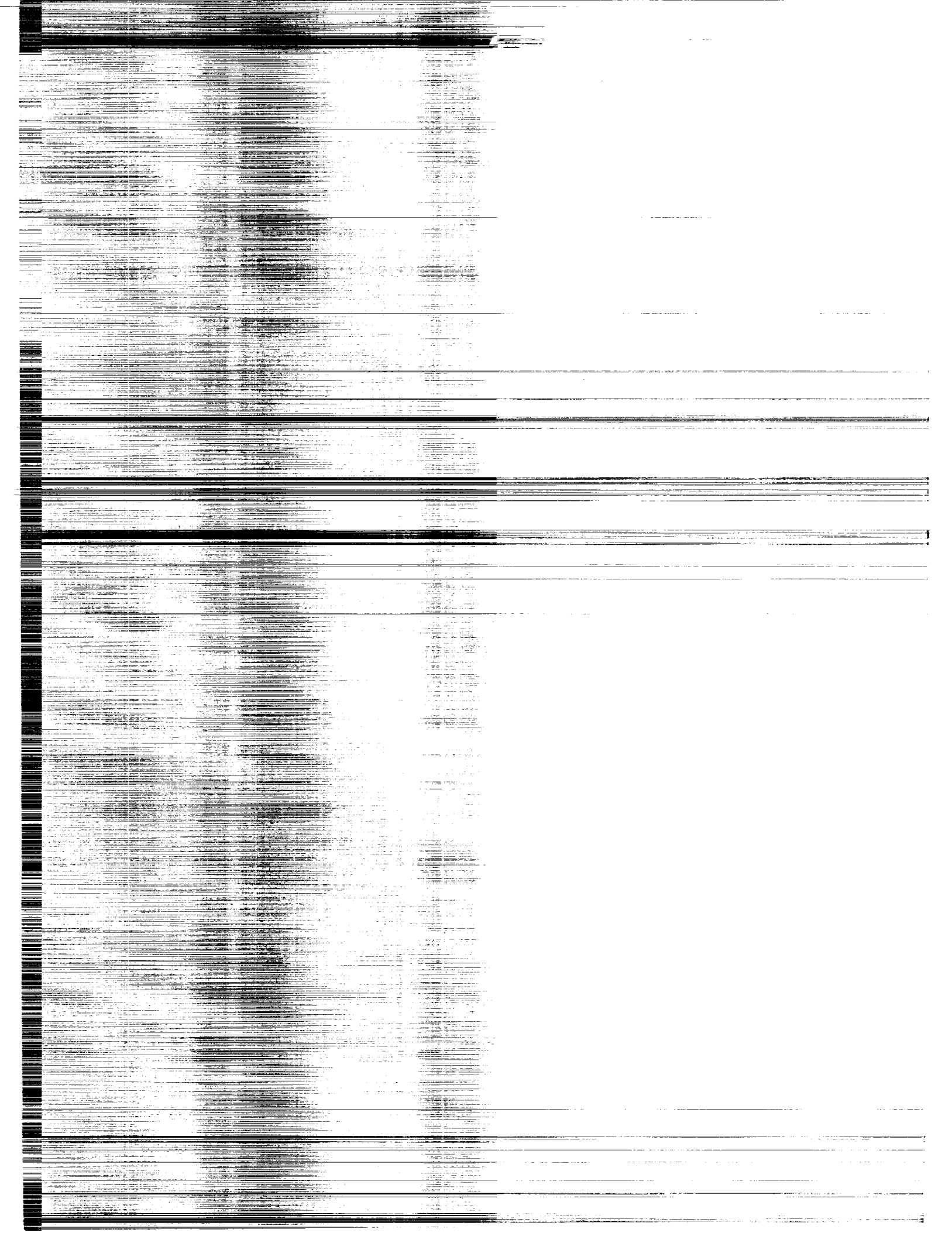

NASA Technical Memorandum 4362

Quasi-Elastic Nuclear Scattering at High Energies

Francis A. Cucinotta, Lawrence W. Townsend,
and John W. Wilson
Langley Research Center
Hampton, Virginia

National Aeronautics and
Space Administration
Office of Management
Scientific and Technical
Information Program
1992

Abstract

The quasi-elastic scattering of two nuclei is considered in the high-energy optical model. Energy loss and momentum transfer spectra for projectile ions are evaluated in terms of an inelastic multiple-scattering series corresponding to multiple knockout of target nucleons. The leading-order correction to the coherent projectile approximation is evaluated. Calculations with uncorrelated wave functions are compared with experimental results.

Introduction

The assessment of radiation risk to astronauts from cosmic radiation is currently an area of active investigation. Predictions of biological damage will ultimately require a knowledge of the particle fluence spectra at the endpoint of interest. In turn, these particle fluence spectra are determined from charged-particle transport codes that must contain a description of all important physical processes that occur as the incident ions and subsequent generation fragment nuclei pass through natural and protective radiation shielding. A theoretical model for the prediction of fragmentation cross sections is extremely useful, as it cannot be expected that enough experiments will be performed for all the collision pairs and energies of interest in cosmic ray studies. Experimental data are most often in the form of inclusive measurements where a single reaction product is typically detected in a many-particle final state. Although several mechanisms may lead to the single product, models must be compared with the inclusive measurements for validation.

The inelastic collision of two nuclei at intermediate or high energies is often described as a two-step process. The first step includes multiple scatterings between projectile and target nucleons leading to the knockout of nucleons and clusters, the production of particles, and the deposition of energy. The second step involves the cascade of initially struck particles within their host nuclei and the de-excitation of the nuclear systems, which may proceed through particle emission. Recently, we have considered inclusive heavy-ion scattering using the high-energy optical model (refs. 1 and 2). The multiple scatterings between projectile and target nucleons can be divided into elastic and inelastic collision terms corresponding to a distortion effect and the knockout of nucleons, respectively. Calculations (ref. 2) with the independent particle model (IPM) show that even for large collision pairs, the number of inelastic collisions that occur is quite small, usually two to four. Although correlation effects may be important corrections to the IPM, especially for cluster knockout, the rapid convergence in the number of inelastic collisions favors a "doorway" picture of heavy-ion fragmentation. In the doorway picture the first step involves only a small number of knocked-out nucleons, with the subsequent motion of these particles and nuclear de-excitation leading to the large number of final fragmentation channels observed in experiments.

In our previous work (refs. 1 and 2) the cross-section distribution in total momentum transfer was considered. Herein, we extend this work in order to evaluate the energy loss cross section of the projectile in inclusive scattering. The relationship of the projectile energy loss to the target response function and excitation energy is considered and the effects of multiple inelastic scatterings are treated. The correction to the coherent projectile assumption (ref. 1) is evaluated to leading order. Previous calculations in high-energy formulations (refs. 3 to 5) have considered only elementary projectiles and usually assume a zero-range two-body interaction (ref. 4) or a factorization approximation (ref. 3). In this work only forward-peaked wave functions are assumed in the evaluation of higher order terms. The model presented herein is immediately applicable to the development of nuclear transport codes for bulk shielding materials, as is

illustrated with calculations of energy loss distributions for protons, ^{4}He and ^{16}O in common shielding materials. The methods developed herein are expected to lead to an improved description of the first step of heavy-ion fragmentation.

Multiple Inelastic Collision Series

In the eikonal coupled channels (ECC) model (refs. 6 to 8) the matrix of scattering amplitudes for all possible projectile-target transitions is given by

$$\overline{f}(\mathbf{q}) = \frac{ik}{2\pi}\hat{Z}\int d^2b\, e^{i\mathbf{q}\cdot\mathbf{b}}\left[e^{i\overline{\chi}(\mathbf{b})} - \overline{1}\right] \tag{1}$$

where barred quantities represent matrices, $\mathbf{b}$ is the impact parameter vector, $\mathbf{q}$ the momentum transfer vector, and k the projectile-target relative wave number. In equation (1), $\hat{Z}$ is an ordering operator for the z-coordinate, which is necessary only when noncommuting two-body interactions are considered. The eikonal phase elements are defined by matrix elements of arbitrary projectile-target states of the following operator (for commuting two-body interactions):

$$\hat{\chi}(\mathbf{b}) = \frac{1}{2\pi k_{\mathrm{NN}}}\sum_{\alpha,j}\int d^2q\, e^{i\mathbf{q}\cdot\mathbf{b}}\, e^{-i\mathbf{q}\cdot\mathbf{s}_\alpha}\, e^{i\mathbf{q}\cdot\mathbf{s}_j} f_{\mathrm{NN}}(\mathbf{q}) \tag{2}$$

where α and j label the projectile and target constituents, respectively, $\mathbf{s}$ is the projection of the internal nuclear coordinate onto the impact parameter plane, f_{NN} is the nucleon-nucleon scattering amplitude, and k_{NN} is the nucleon-nucleon relative wave number.

In treating inelastic scattering we assume the off-diagonal terms in $\overline{\chi}$, denoted by $\overline{\chi}_O$, are small compared with the diagonal ones, $\overline{\chi}_D$, and then expand $\overline{f}$ in powers of $\overline{\chi}_O$:

$$\overline{f}(\mathbf{q}) = \frac{-ik}{2\pi}\int d^2b\, e^{i\mathbf{q}\cdot\mathbf{b}} e^{i\overline{\chi}_D(\mathbf{b})}\sum_{m=1}\left\{\frac{[i\overline{\chi}_O(\mathbf{b})]^m}{m!}\right\} \tag{3}$$

We also will make the assumption that the diagonal terms are all represented by the ground-state elastic phase χ. Using equation (3) we sum over target final states X (continuum) to find the inclusive angular distribution for the projectile when its mass remains unchanged as

$$\left(\frac{d\sigma}{d\Omega}\right)_{\mathrm{IN}} = \frac{k^2}{(2\pi)^2}\int d^2b\, d^2b'\, e^{i\mathbf{q}\cdot(\mathbf{b}-\mathbf{b}')}\, e^{i\left[\chi(\mathbf{b})-\chi^\dagger(\mathbf{b}')\right]}$$
$$\times\sum_{X\neq 0}\sum_{m=1}\frac{1}{(m!)^2} < O_P O_T|\,[i\hat{\chi}(\mathbf{b})]^m\,|O_P X >$$
$$\times < XO_P|\left[-i\hat{\chi}^\dagger(\mathbf{b}')\right]^m|O_P O_T > \tag{4}$$

Equation (4) allows only for a study of the momentum transfer spectra of the projectile. In considering the projectile energy loss, energy conservation must be treated. With continuum states used for the target final state, energy conservation leads to

$$\left(\frac{d^2\sigma}{d\Omega\, dE_{P'}}\right)_{\mathrm{IN}} = \frac{k^2}{(2\pi)^2}\int d^2b\, d^2b'\, e^{i\mathbf{q}\cdot(\mathbf{b}-\mathbf{b}')}\, e^{i\left[\chi(\mathbf{b})-\chi^\dagger(\mathbf{b}')\right]}\sum_{m=1}^{A_T} W_m(\mathbf{b},\mathbf{b}',w) \tag{5}$$

and

$$\left(\frac{d\sigma}{dE_{P'}}\right)_{\mathrm{IN}} = \int d^2b\, e^{-2\mathrm{Im}[\chi(\mathbf{b})]} \sum_{m=1}^{A_T} W_m\left(\mathbf{b},\mathbf{b},w\right) \tag{6}$$

where $E_{P'}$ is the energy of the projectile in the final state, w is the projectile energy loss, and we define

$$W_m\left(\mathbf{b},\mathbf{b}',w\right) = \frac{1}{(m!)^2}\int \prod_{j=1}^{m}\left[\frac{d\mathbf{k}_j}{(2\pi)^2}\right]\delta\left(E_f - E_i\right) < O_P O_T|\left[\hat{\chi}\left(\mathbf{b}\right)\right]^m|O_P\mathbf{k}_j >$$

$$< \mathbf{k}_j O_P\left|\left[\hat{\chi}^\dagger\left(\mathbf{b}'\right)\right]^m\right|O_P O_T > \tag{7}$$

where $\mathbf{k}_j$ is the wave number vector of a knocked-out target nucleon.

The inelastic collision series of equation (5) is expected to converge fairly rapidly, and in the next section we consider evaluating this series for an uncorrelated target wave function and using plane-wave states for knocked-out nucleons. First, we briefly consider the lowest order term and its relationship to the target response function. The first inelastic term is

$$W_1\left(\mathbf{b},\mathbf{b}',w\right) = \int d^2q\, d^2q'\, e^{i\mathbf{q}\cdot\mathbf{b}}\, e^{-i\mathbf{q}'\cdot\mathbf{b}'} F\left(\mathbf{q}\right) F\left(-\mathbf{q}'\right) f_{\mathrm{NN}}\left(\mathbf{q}\right) f^\dagger_{\mathrm{NN}}\left(\mathbf{q}'\right)$$

$$\times \int \frac{d\mathbf{k}}{(2\pi)^2}\,\delta\left(E_f - E_i\right) < O_T\left|\sum_j e^{i\mathbf{q}\cdot\mathbf{s}_j}\right|\mathbf{k} >< \mathbf{k}\left|\sum_j e^{-i\mathbf{q}'\cdot\mathbf{s}'_j}\right|O_T > \tag{8}$$

If we neglect target recoil we can write

$$\delta\left(E_f - E_i\right) = \frac{-1}{\pi}\mathrm{Im}\left(\frac{1}{w - E_{\mathbf{k}} + i\eta} - \frac{1}{w + E_{\mathbf{k}} + i\eta}\right) \tag{9}$$

and then

$$W_1\left(\mathbf{b},\mathbf{b}',w\right) = \int d^2q\, d^2q'\, e^{i\mathbf{q}\cdot\mathbf{b}}\, e^{-i\mathbf{q}'\cdot\mathbf{b}'} F\left(\mathbf{q}\right) F\left(-\mathbf{q}'\right) f_{\mathrm{NN}}\left(\mathbf{q}\right) f^\dagger_{\mathrm{NN}}\left(\mathbf{q}'\right)$$

$$\times \frac{-1}{\pi} R\left(\mathbf{q},\mathbf{q}',w\right) \tag{10}$$

where the target response function is

$$R\left(\mathbf{q},\mathbf{q}',w\right) = \int \frac{d\mathbf{k}}{(2\pi)^2}\sum_{jj'} < O_T|e^{i\mathbf{q}\cdot\mathbf{s}_j}|\mathbf{k} >< \mathbf{k}|e^{-i\mathbf{q}'\cdot\mathbf{s}'_j}|O_T >$$

$$\times \left(\frac{1}{w - E_{\mathbf{k}} + i\eta} - \frac{1}{w + E_{\mathbf{k}} + i\eta}\right) \tag{11}$$

Only the $j' = j$ terms contribute for nonzero w, and we neglect the $j \neq j'$ terms since bound states dominate for small w. The plane-wave impulse approximation (PWIA) assumes that $\chi \approx 0$ and that only the $m = 1$ term contributes, such that

$$\frac{d^2\sigma}{d\Omega\, dE_{P'}} \approx \frac{k^2}{k^2_{\mathrm{NN}}} A_P^2 A_T F^2\left(\mathbf{q}\right)\frac{d\sigma}{d\Omega_{\mathrm{NN}}}\left[\frac{-1}{\pi} R\left(\mathbf{q},\mathbf{q},w\right)\right] \tag{12}$$

We also note that in nuclear matter, translation invariance implies (ref. 9)

$$R\left(\mathbf{q},\mathbf{q}',w\right)=R\left(\mathbf{q},\mathbf{q}',w\right)\delta\left(\mathbf{q}-\mathbf{q}'\right) \tag{13}$$

which leads to some simplification in distorted wave calculations. Bertsch and Esbensen (refs. 10 to 12) have introduced a surface response model in which the PWIA is assumed; however, eikonal waves are introduced into the response operator and provide localization to the nuclear surface. This approach works quite well when multiple inelastic collisions do not contribute. For large momentum transfer and larger projectiles these higher order terms may become important and are treated next.

Collision Terms

In evaluating the collision terms W_m, we assume an uncorrelated wave function for the target and plane waves for continuum states. The inclusion of final-state interactions occurs in the transition form factors of the target discussed below. The projectile motion is treated in the coherent approximation following reference 1 and the leading-order correction is considered.

The first collision term is written as

$$W_1\left(\mathbf{b},\mathbf{b}',w\right)=\frac{A_P^2A_T}{\left(2\pi k_{\mathrm{NN}}\right)^2}\int d^2q\,d^2q'\,e^{i\mathbf{q}\cdot\mathbf{b}}\;e^{-i\mathbf{q}'\cdot\mathbf{b}'}F\left(\mathbf{q}\right)F\left(\mathbf{q}'\right)$$

$$\times f_{\mathrm{NN}}\left(\mathbf{q}\right)f_{\mathrm{NN}}^{\dagger}\left(\mathbf{q}'\right)\int\frac{d^2k}{\left(2\pi\right)^2}\,\delta\left(w-E_{\mathbf{k}}\right)G_{O_T\mathbf{k}}\left(\mathbf{q}\right)G_{\mathbf{k}O_T}^{\dagger}\left(\mathbf{q}'\right) \tag{14}$$

It is helpful to change variables as follows:

$$\boldsymbol{\alpha}=\frac{1}{2}\left(\mathbf{q}+\mathbf{q}'\right) \tag{15}$$

$$\boldsymbol{\beta}=\mathbf{q}-\mathbf{q}' \tag{16}$$

$$\mathbf{x}=\mathbf{s}-\mathbf{s}' \tag{17}$$

$$\mathbf{y}=\frac{1}{2}\left(\mathbf{s}+\mathbf{s}'\right) \tag{18}$$

$$\mathbf{R}=\mathbf{b}-\mathbf{b}' \tag{19}$$

$$\mathbf{S}=\frac{1}{2}\left(\mathbf{b}+\mathbf{b}'\right) \tag{20}$$

such that

$$W_1\left(\mathbf{R},\mathbf{S},w\right)=\frac{A_P^2A_T}{\left(2\pi k_{\mathrm{NN}}\right)^2}\int d^2\alpha\,d^2\beta\;e^{i\boldsymbol{\alpha}\cdot\mathbf{R}}\;e^{i\boldsymbol{\beta}\cdot\mathbf{S}}A\left(\boldsymbol{\alpha}+\frac{\boldsymbol{\beta}}{2}\right)\;A^{\dagger}\left(\boldsymbol{\alpha}-\frac{\boldsymbol{\beta}}{2}\right)$$

$$\times R_1\left(\boldsymbol{\alpha},\boldsymbol{\beta},w\right) \tag{21}$$

where we have defined

$$A\left(\mathbf{q}\right)=F\left(\mathbf{q}\right)f_{\mathrm{NN}}\left(\mathbf{q}\right) \tag{22}$$

and

$$R_1\left(\boldsymbol{\alpha},\boldsymbol{\beta},w\right)=\int\frac{d\mathbf{k}}{\left(2\pi\right)^2}\,\delta\left(w-E_{\mathbf{k}}\right)\;G_{O_T\mathbf{k}}\left(\boldsymbol{\alpha}+\frac{\boldsymbol{\beta}}{2}\right)\;G_{\mathbf{k}O_T}^{\dagger}\left(\boldsymbol{\alpha}-\frac{\boldsymbol{\beta}}{2}\right) \tag{23}$$

Following Krimm et al. (ref. 3), we can formally treat the delta function in equation (23) by introducing a Fourier transform pair:

$$R_1(\boldsymbol{\alpha},\boldsymbol{\beta},w) = \int_{-\infty}^{\infty} \frac{dt}{2\pi}\, e^{iwt} \tilde{R}_1(\boldsymbol{\alpha},\boldsymbol{\beta},t) \tag{24}$$

$$\tilde{R}_1(\boldsymbol{\alpha},\boldsymbol{\beta},t) = \int_{-\infty}^{\infty} dw\, e^{-iwt} R_1(\boldsymbol{\alpha},\boldsymbol{\beta},w) \tag{25}$$

Then,

$$\tilde{R}_1(\boldsymbol{\alpha},\boldsymbol{\beta},t) = \int \frac{d\mathbf{k}}{(2\pi)^2}\, e^{-iE_{\mathbf{k}}t}\, G_{O_T\mathbf{k}}\left(\boldsymbol{\alpha}+\frac{\boldsymbol{\beta}}{2}\right)\, G^{\dagger}_{\mathbf{k}O_T}\left(\boldsymbol{\alpha}-\frac{\boldsymbol{\beta}}{2}\right) \tag{26}$$

For a nonrelativistic nucleon we have

$$E_{\mathbf{k}} = \frac{\mathbf{k}^2}{2m_N} + \epsilon_{B_1} \tag{27}$$

where ϵ_{B_1} is the binding energy. Equation (26) then becomes, with the assumption of plane waves for the target final state in $G_{O_T\mathbf{k}}$,

$$\begin{aligned}\tilde{R}_1(\boldsymbol{\alpha},\boldsymbol{\beta},t) = \int \frac{d\mathbf{k}}{(2\pi)^2}\, d\mathbf{x}\, d\mathbf{y}\, e^{-i\epsilon_{B_1}t}\, e^{-\mathbf{k}^2 t/2m_N}\, e^{i\boldsymbol{\alpha}\cdot\mathbf{x}}\, e^{i\boldsymbol{\beta}\cdot\mathbf{y}}\, e^{i\mathbf{k}\cdot\mathbf{x}} \\ \times \Phi\left(\mathbf{y}+\frac{\mathbf{x}}{2}\right)\Phi^{\dagger}\left(\mathbf{y}-\frac{\mathbf{x}}{2}\right)\end{aligned} \tag{28}$$

where Φ is the single-particle wave function of the target ground state. After two integrations we find from equations (28) and (24) that

$$R_1(\boldsymbol{\alpha},\boldsymbol{\beta},w) = \left\{ \begin{array}{ll} \frac{m_N}{2\pi}\int d\mathbf{x}\, d\mathbf{y}\, e^{i\boldsymbol{\alpha}\cdot\mathbf{x}} & \\ \quad \times e^{i\boldsymbol{\beta}\cdot\mathbf{y}}\, J_o\left(\sqrt{2m_N\left(w-\epsilon_{B_1}\right)x^2}\right) & \\ \quad \times \Phi\left(\mathbf{y}+\frac{\mathbf{x}}{2}\right)\Phi^{\dagger}\left(\mathbf{y}-\frac{\mathbf{x}}{2}\right) & \left(w \geq \epsilon_{B_1}\right) \\ 0 & \left(w < \epsilon_{B_1}\right) \end{array} \right\} \tag{29}$$

The second collision term is found in a similar fashion to be

$$\begin{aligned} W_2(\mathbf{R},\mathbf{S},w) = \frac{A_P^4 A_T^2}{4\left(2\pi k_{\mathrm{NN}}\right)^4} \int d^2\alpha_1\, d^2\alpha_2\, d^2\beta_1\, d^2\beta_2\, e^{i(\boldsymbol{\alpha}_1+\boldsymbol{\alpha}_2)\cdot\mathbf{R}} \\ \times e^{i(\boldsymbol{\beta}_1+\boldsymbol{\beta}_2)\cdot\mathbf{S}}\, A\left(\boldsymbol{\alpha}_1+\frac{\boldsymbol{\beta}_1}{2}\right)\, A^{\dagger}\left(\boldsymbol{\alpha}_1-\frac{\boldsymbol{\beta}_1}{2}\right)\, A\left(\boldsymbol{\alpha}_2+\frac{\boldsymbol{\beta}_2}{2}\right) \\ \times A^{\dagger}\left(\boldsymbol{\alpha}_2-\frac{\boldsymbol{\beta}_2}{2}\right)\, R_2(\boldsymbol{\alpha}_1,\boldsymbol{\alpha}_2,\boldsymbol{\beta}_1,\boldsymbol{\beta}_2,w) \end{aligned} \tag{30}$$

where

$$R_2(\boldsymbol{\alpha}_1,\boldsymbol{\alpha}_2,\boldsymbol{\beta}_1,\boldsymbol{\beta}_2,w)=\left\{\begin{array}{ll}\frac{m_N^2}{(2\pi)^2}\int d^2x_1\,d^2x_2\,d^2y_1\,d^2y_2\,e^{i\boldsymbol{\alpha}_1\cdot\mathbf{x}_1}e^{i\boldsymbol{\alpha}_2\cdot\mathbf{x}_2}e^{i\boldsymbol{\beta}_1\cdot\mathbf{y}_1}e^{i\boldsymbol{\beta}_2\cdot\mathbf{y}_2} & \\ \quad\times\Phi\left(\mathbf{y}_1+\frac{\mathbf{x}_1}{2}\right)\Phi^\dagger\left(\mathbf{y}_1-\frac{\mathbf{x}_1}{2}\right)\Phi\left(\mathbf{y}_2+\frac{\mathbf{x}_2}{2}\right)\Phi^\dagger\left(\mathbf{y}_2-\frac{\mathbf{x}_2}{2}\right) & \\ \quad\times\frac{2\left(w-\epsilon_{B_2}\right)}{\sqrt{2m_N\left(w-\epsilon_{B_2}\right)\left(x_1^2+x_2^2\right)}}\,J_1\left[\sqrt{2m_N\left(w-\epsilon_{B_2}\right)\left(x_1^2+x_2^2\right)}\right] & \left(w\geq\epsilon_{B_2}\right)\\ 0 & \left(w<\epsilon_{B_2}\right)\end{array}\right\} \tag{31}$$

With similar coordinate changes as those described above, the mth order collision term is

$$\begin{aligned}W_m(\mathbf{R},\mathbf{S},w)=&\frac{A_P^{2m}A_T^m}{(m!)^2(2\pi k_{\mathrm{NN}})^{2m}}\int\prod_{j=1}^{m}\Big[d^2\alpha_j\,d^2\beta_j\\&\times e^{i\boldsymbol{\alpha}_j\cdot\mathbf{R}}\,e^{i\boldsymbol{\beta}_j\cdot\mathbf{S}}\,A_j\left(\boldsymbol{\alpha}_j+\frac{\boldsymbol{\beta}_j}{2}\right)\,A_j^\dagger\left(\boldsymbol{\alpha}_j-\frac{\boldsymbol{\beta}_j}{2}\right)\Big]\\&\times R_m(\boldsymbol{\alpha}_1,\boldsymbol{\alpha}_2,\ldots,\boldsymbol{\alpha}_m,\boldsymbol{\beta}_1,\boldsymbol{\beta}_2,\ldots,\boldsymbol{\beta}_m,w)\end{aligned} \tag{32}$$

where

$$R_m(\boldsymbol{\alpha}_1,\boldsymbol{\alpha}_2,\ldots,\boldsymbol{\alpha}_m,\boldsymbol{\beta}_1,\boldsymbol{\beta}_2,\ldots,\boldsymbol{\beta}_m,w)=\left\{\begin{array}{ll}\frac{m_N^m}{(2\pi)^m}\int\prod_{j=1}^{m}\left[d^2x_j\,d^2y_j\,e^{i\boldsymbol{\alpha}_j\cdot\mathbf{x}_j}\,e^{i\boldsymbol{\beta}_j\cdot\mathbf{y}_j}\right. & \\ \quad\left.\times\Phi\left(\mathbf{y}_j+\frac{\mathbf{x}_j}{2}\right)\Phi^\dagger\left(\mathbf{y}_j-\frac{\mathbf{x}_j}{2}\right)\right] & \\ \quad\times\frac{2^{m-1}\left(w-\epsilon_{B_m}\right)^{m-1}}{\left[2m_N\left(w-\epsilon_{B_m}\right)\sum_{j=1}^{m}x_j^2\right]^{(m-1)/2}} & \\ \quad\times J_{m-1}\left(\sqrt{2m_N\left(w-\epsilon_{B_m}\right)\sum_{j=1}\,x_j^2}\right) & \left(w\geq\epsilon_{B_m}\right)\\ 0 & \left(w<\epsilon_{B_m}\right)\end{array}\right\} \tag{33}$$

We next look for a simplification of the terms for $m>1$.

The mth order Bessel function is given by (ref. 13)

$$J_m(x)=\frac{1}{m!}\left(\frac{x}{2}\right)^m\left[1-\frac{1}{m+1}\left(\frac{x}{2}\right)^2+\frac{1}{(m+1)(m+2)}\frac{1}{2!}\left(\frac{x}{2}\right)^4-\ldots+\ldots\right] \tag{34}$$

We introduce the approximation

$$\frac{J_{m-1}\left(\xi_m\sqrt{\sum_{j=1}^{m}x_j^2}\right)}{\left(\xi_m\sqrt{\sum_{j=1}^{m}x_j^2}\right)^{m-1}}\approx\frac{1}{(m-1)!\,2^{m-1}}\prod_{j=1}^{m}J_o\left(\frac{\xi_m x_j}{2^{(m-1)/2}}\right)+O\left(\xi_m^4x_j^4\right) \tag{35}$$

where

$$\xi_m=\sqrt{2m_N\left(w-\epsilon_{B_m}\right)} \tag{36}$$

such that

$$R_m(\boldsymbol{\alpha}_1,\boldsymbol{\alpha}_2,\ldots,\boldsymbol{\alpha}_m,\boldsymbol{\beta}_1,\boldsymbol{\beta}_2,\ldots,\boldsymbol{\beta}_m,w)\approx\frac{\left(w-\epsilon_{B_m}\right)^{m-1}}{(m-1)!}\prod_{j=1}^{m}R_1\left(\boldsymbol{\alpha}_j,\boldsymbol{\beta}_j,\frac{\xi_m}{2^{(m-1)/2}}\right) \tag{37}$$

and

$$W_m(\mathbf{R},\mathbf{S},w)=\frac{(w-\epsilon_{B_m})^{m-1}}{(m-1)!\,(m!)^2}\left[W_1\left(\mathbf{R},\mathbf{S},\frac{\xi_m}{2^{(m-1)/2}}\right)\right]^m \tag{38}$$

Equation (35) is expected to be a useful approximation since the wave functions are peaked at $\mathbf{x}_j=0$. Also, since $\epsilon_{B_1}<\epsilon_{B_2}<\ldots<\epsilon_{B_m}$ and successive terms in the collision series dominate as w increases, ξ_m should not be too large in the region of interest. We then have for the energy loss spectra (eq. (5))

$$\left(\frac{d^2\sigma}{d\Omega\,dE_{P'}}\right)_{\rm IN}=\frac{k^2}{(2\pi)^2}\int d^2R\,d^2S\,e^{i\mathbf{q}\cdot\mathbf{R}}\;e^{i\left\{\chi[\mathbf{R}+(\mathbf{S}/2)]-\chi^\dagger[\mathbf{R}-(\mathbf{S}/2)]\right\}}$$
$$\times\sum_{m=1}^{A_T}\frac{(w-\epsilon_{B_m})^{m-1}}{(m-1)!\,(m!)^2}\left[W_1\left(\mathbf{R},\mathbf{S},\frac{\xi_m}{2^{(m-1)/2}}\right)\right]^m \tag{39}$$

and

$$\frac{d\sigma}{dE_{P'}}=\int d^2S\,e^{-2{\rm Im}[\chi(\mathbf{S})]}$$
$$\times\sum_{m=1}^{A_T}\frac{(w-\epsilon_{B_m})^{m-1}}{(m-1)!\,(m!)^2}\left[W_1\left(0,\mathbf{S},\frac{\xi_m}{2^{(m-1)/2}}\right)\right]^m \tag{40}$$

The coherent approximation assumes the projectile remains in the ground state throughout the scattering. The leading-order correction to the coherent terms occurs in W_2 and corresponds to the following replacement (from eq. (55) of ref. 1):

$$A_P^4F\left(\boldsymbol{\alpha}_1+\frac{\boldsymbol{\beta}_1}{2}\right)\;F\left(\boldsymbol{\alpha}_1-\frac{\boldsymbol{\beta}_1}{2}\right)F\left(\boldsymbol{\alpha}_2+\frac{\boldsymbol{\beta}_2}{2}\right)\;F\left(\boldsymbol{\alpha}_2-\frac{\boldsymbol{\beta}_2}{2}\right)$$
$$\to A_P^2\left\{\left[F(2\boldsymbol{\alpha}_1)+(A_P-1)\;F\left(\boldsymbol{\alpha}_1+\frac{\boldsymbol{\beta}_1}{2}\right)\;F\left(\boldsymbol{\alpha}_1-\frac{\boldsymbol{\beta}_2}{2}\right)\right]\right.$$
$$\left.\times\left[F(2\boldsymbol{\alpha}_2)+(A_P-1)\;F\left(\boldsymbol{\alpha}_2+\frac{\boldsymbol{\beta}_2}{2}\right)\;F\left(\boldsymbol{\alpha}_2-\frac{\boldsymbol{\beta}_2}{2}\right)\right]\right\} \tag{41}$$

which physically allows the projectile to dissociate in the intermediate state. Further modifications, which are not included herein, are necessary when correlation effects are treated. Next we consider model inputs and application of the above formalism.

Calculations

We next discuss physical inputs necessary for evaluation of the cross sections of equations (39) and (40). We employ a two-body amplitude of the form

$$f_{\rm NN}(\mathbf{q})=\frac{\sigma(\rho+i)\,k_{\rm NN}}{4\pi}\;e^{-Bq^2/2} \tag{42}$$

where the spin-isospin averaged energy-dependent parameters are the two-body cross section σ, the ratio of the real to imaginary parts of the forward amplitude ρ, and the diffractive slope parameter B.

For nuclei with mass number $A \leq 16$ we use harmonic oscillator shell model wave functions. For s-shell nucleons (ref. 14),

$$\Phi_s(\mathbf{r}) = \left(\frac{1}{\pi a}\right)^{3/4} e^{-r^2/2a} \tag{43}$$

and for p-shell nucleons

$$\Phi_p(\mathbf{r}) = \left(\frac{1}{\pi a}\right)^{3/4} \sqrt{2/a}\, r_m\, e^{-r^2/2a} \tag{44}$$

where a is related to the nuclear radius R by $a = R^2$ and the internal coordinate is expressed in terms of spherical coordinates as

$$r_m = \begin{cases} \frac{1}{\sqrt{2}}(r_1 \pm i r_2) & (m = 1 \text{ and } 2) \\ r_3 & (m = 3) \end{cases} \tag{45}$$

The s-shell and p-shell probabilities are given by

$$C_s = \frac{4}{A} \tag{46}$$

and

$$C_p = \frac{A-4}{A} \tag{47}$$

with $C_s = 1$ and $C_p = 0$ for $A \leq 4$.

The projectile form factors are evaluated from equations (43) and (44) as

$$F(\mathbf{q}) = \int \sum_{s,p} C_{s,p} |\Phi_{s,p}(\mathbf{r})|^2 \, d^3r \tag{48}$$

The functions W_1 (eq. (21)) and R_1 (eq. (29)) are now found after some effort.

Results and Discussion

Experiments with 800-MeV protons (ref. 15) were performed with several targets to study the quasi-elastic peak and extend to regions of energy loss corresponding to pion production. Herein we consider only the quasi-elastic and dip regions of the data. In figures 1 to 6 we show comparisons of calculations with experimental data for ^{7}Li and ^{12}C at several scattering angles. The dotted line is for the single-knockout term, the dashed line is for the single- and double-knockout terms, and the solid line includes all contributions up to $m = 4$. The fourth-order term makes only a small contribution for both targets. Because of our neglect of target recoil and any target excitation energy, the position of the peak of the calculated values is shifted to slightly lower energies than those of the experimental values. Following reference 4 we corrected this shortcoming by performing calculations at $w \rightarrow w - \epsilon_{B_1}$. The position of the quasi-elastic peak is then well reproduced by the calculations. In the dip region, pion production channels prevent a direct comparison with the data at this energy. The spin dependence of the nucleon-nucleon amplitudes also affects the results in this region.

In figures 7 to 10 we show comparisons of calculations at various angles for ^{4}He-^{4}He scattering at 1.05 GeV/amu with data from reference 16. The solid line shows the $m = 1$ to 4 terms with the $m = 2$ term correction for incoherent projectile motion of equation (41) included. The dashed line neglects this correction, the dash-dot line is for the $m = 1$ and 2 terms, and the dotted line is for just the $m = 1$ term. The coherent projectile assumption decreases the contribution from

the second collision term. The comparisons with experimental values in figures 9 and 10 are at scattering angles corresponding to momentum transfers where the Gaussian wave functions used are known to have insufficient strength. In figure 11 we show the angle-integrated cross section for α-α scattering. The dashed line is the single knockout and the solid line is the complete series. Multiple nucleon knockout represents a large correction for large energy loss.

In figures 12 and 13 we show inclusive ^{4}He scattering on ^{16}O at 1 GeV/amu for scattering angles of 1° and 4°, respectively. The dashed line is for the first inelastic collision term only, the dash-dot line is for the first and second terms, the dotted line is for the first to third terms, and the solid line is for the sum of the first to fourth inelastic collisions. The higher order terms are more important here than they are for the case of proton projectiles. (See figs. 1 to 6.) In comparing figures 12 and 13 we note that the forward peak in the cross section is an indication that the projectile is unlikely to receive both a large energy loss and a momentum transfer without suffering a change in mass. In figures 14 and 15 we show a similar comparison for ^{16}O scattering on ^{16}O at 1 GeV/amu for scattering angles of 0.5° and 1.0°.

Conclusions

The high-energy optical model is used to describe energy loss spectra of projectile nuclei in high-energy collisions. An inelastic multiple-scattering series is found for inclusive projectile scattering that corresponds to the knockout of target particles. Preliminary calculations are presented for proton, ^{4}He, and ^{16}O projectiles with an approximation to the higher order (>2) inelastic collision terms. Improvements in the model should be the inclusion of final-state interactions of knocked-out target nucleons and the addition of pion production into the calculations of the inelastic spectra. Calculations will also be improved by considering spin-dependent two-body amplitudes and the use of response functions that treat low-lying collective behavior of the target.

NASA Langley Research Center
Hampton, VA 23665-5225
April 9, 1992

References

1. Cucinotta, Francis A.; Townsend, Lawrence W.; Wilson, John W.; and Khandelwal, Govind S.: *Inclusive Inelastic Scattering of Heavy Ions and Nuclear Correlations.* NASA TP-3026, 1990.

2. Cucinotta, Francis A.; Townsend, Lawrence W.; and Wilson, John W.: Inclusive Inelastic Scattering of Heavy Ions in the Independent Particle Model. *J. Phys. G: Nucl. Particle Phys.*, vol. 18, 1992. (To be published.)

3. Krimm, H.; Klar, A.; and Pirner, H. J.: Inelastic Scattering of Fast Particles on Nuclei. *Nucl. Phys.*, vol. A367, no. 3, Sept. 14, 1981, pp. 333 357.

4. Smith, Richard D.; and Wallace, Stephen J.: Spin Observables in Quasi-Elastic Proton-Nucleus Scattering Near 1 GeV. *Phys. Review C*, third ser., vol. 32, no. 5, Nov. 1985, pp. 1654 1666.

5. Azhgirei, L. S.; Vzorov, I. K.; Zhmyrov, V. N.; Ivanov, V. V.; Ignatenko, M. A.; Kuznetsov, A. S.; Meshcheryakov, M. G.; Pak, A. S.; Rasin, S. V.; Stoletov, G. D.; Tarasov, A. V.; and Tseren, Ch.: Nuclear Scattering of Deuterons at 4.3, 6.3, and 8.9 GeV/c. *Sov. J. Nucl. Phys.*, vol. 30, no. 6, Dec. 1979, pp. 818 823.

6. Wilson, John W.: Composite Particle Reaction Theory. Ph.D. Diss., College of William and Mary in Virginia, June 1975.

7. Cucinotta, F. A.; Khandelwal, G. S.; Townsend, L. W.; and Wilson, J. W.: Correlations in α-α Scattering and Semi-Classical Optical Models. *Phys. Lett.*, vol. B223, no. 2, June 8, 1989, pp. 127 132.

8. Cucinotta, Francis A.: Theory of Alpha-Nucleus Collisions at High Energies. Ph.D. Thesis, Old Dominion Univ., 1988.

9. Fetter, Alexander L.; and Walecka, John Dirk: *Quantum Theory of Many-Particle Systems.* McGraw-Hill, Inc., c.1971.

10. Esbensen, H.; and Bertsch, G. F.: Surface Response of Fermi Liquids. *Ann. Phys.*, vol. 157, 1984, pp. 255 281.

11. Bertsch, G. F.; and Scholten, O.: Forward-Angle Inelastic Scattering. *Phys. Review C,* third ser., vol. 25, no. 2, Feb. 1982, pp. 804 812.

12. Esbensen, H.; Toki, H.; and Bertsch, G. F.: Surface Effects on the Isovector Spin Response Induced by High Energy Protons. *Phys. Review C,* third ser., vol. 31, no. 5, May 1985, pp. 1816 1820.

13. Mathews, Jon; and Walker, R. L.: *Mathematical Methods of Physics,* Second ed. W. A. Benjamin, Inc., c.1970.

14. Smith, Richard Daniel: Spin Observables in Inelastic Proton-Nucleus Scattering at Intermediate Energy. Ph.D. Diss., Univ. of Maryland, 1984.

15. Chrien, R. E.; Krieger, T. J.; Sutter, R. J.; May, M.; Palevsky, H.; Stearns, R. L.; Kozlowski, T.; and Bauer, T.: Proton Spectra From 800 MeV Protons on Selected Nuclides. *Phys. Review C,* third ser., vol. 21, no. 3, Mar. 1980, pp. 1014 1029.

16. Banaigs, J.; Berger, J.; Berthet, P.; Bizard, G.; Boivin, M.; De Sanctis, M.; Duflo, J.; Fabbri, F. L.; Frascaria, R.; Goldzahl, L.; Picozza, P.; Plouin, F.; and Satta, L.: Inelastic Scattering of α Particles on Light Nuclei at $P_\alpha = 7.0$ GeV/c. *Phys. Review C,* third ser., vol. 35, no. 4, Apr. 1987, pp. 1416 1424.

Symbols

A_P	mass number of projectile nucleus
A_T	mass number of target nucleus
$\mathbf{b}$	impact parameter vector
c	speed of light
E_f	total final energy
E_i	total initial energy
$E_{\mathbf{k}}$	energy of outgoing nucleon
$E_{P'}$	energy of projectile in final state
F	projectile one-particle form factor
f_{NN}	nucleon-nucleon scattering amplitude
G	target transition form factor
j	target constituent index
k	projectile-target relative wave number
$\mathbf{k}$	wave number vector
k_{NN}	nucleon-nucleon relative wave number
m_N	nucleon mass
$\|O_P>$	projectile initial state vector
$\|O_T>$	target initial state vector
p	momentum
$\mathbf{q}$	momentum transfer vector
$\mathbf{R}$	$= \mathbf{b} - \mathbf{b}'$
R_P	projectile matter radius
R_T	target matter radius
$\mathbf{r}$	internal nuclear coordinate vector
$\mathbf{S}$	$= \frac{1}{2}\,(\mathbf{b} + \mathbf{b}')$
$\mathbf{s}$	projection of internal coordinate onto impact parameter plane
$\mathbf{x}$	$= \mathbf{s} - \mathbf{s}'$
$\mathbf{y}$	$= \frac{1}{2}\,(\mathbf{s} + \mathbf{s}')$
α	projectile constituent index
$\boldsymbol{\alpha}$	$= \frac{1}{2}\,(\mathbf{q} + \mathbf{q}')$
$\boldsymbol{\beta}$	$= \mathbf{q} - \mathbf{q}'$
δ	Dirac delta
ϵ_{B_m}	binding energy
σ	cross section

Φ	single-particle wave function of target ground state
χ	ground-state elastic eikonal phase
$\hat{\chi}$	ground-state eikonal phase operator
Ω	solid angle

Subscripts and superscripts:

IN	inclusive
NN	nucleon-nucleon
P	projectile
T	target

Barred quantities represent matrices.

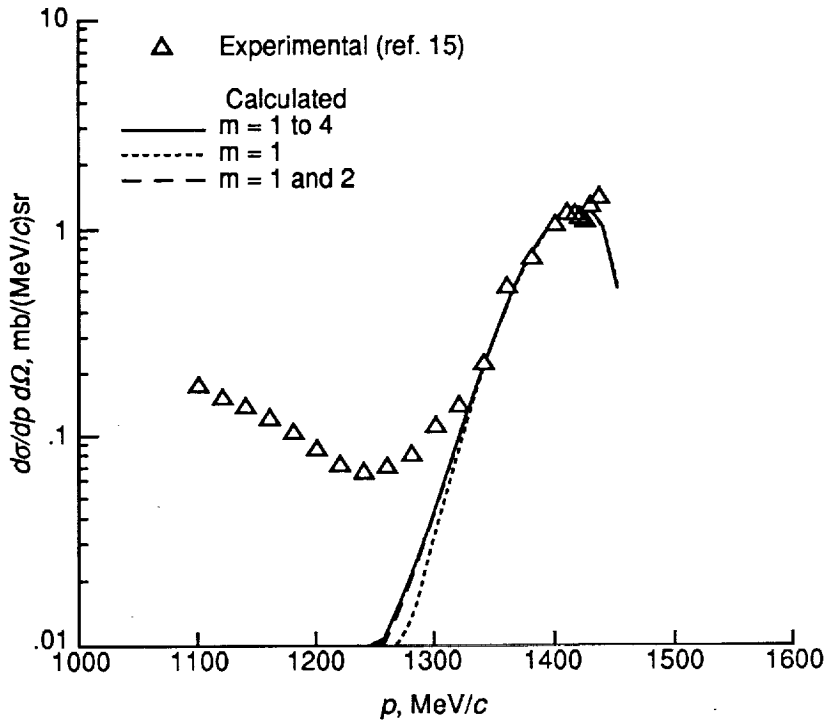

Figure 1. Inclusive proton scattering on ^{7}Li at 800 MeV for scattering angle of 11°.

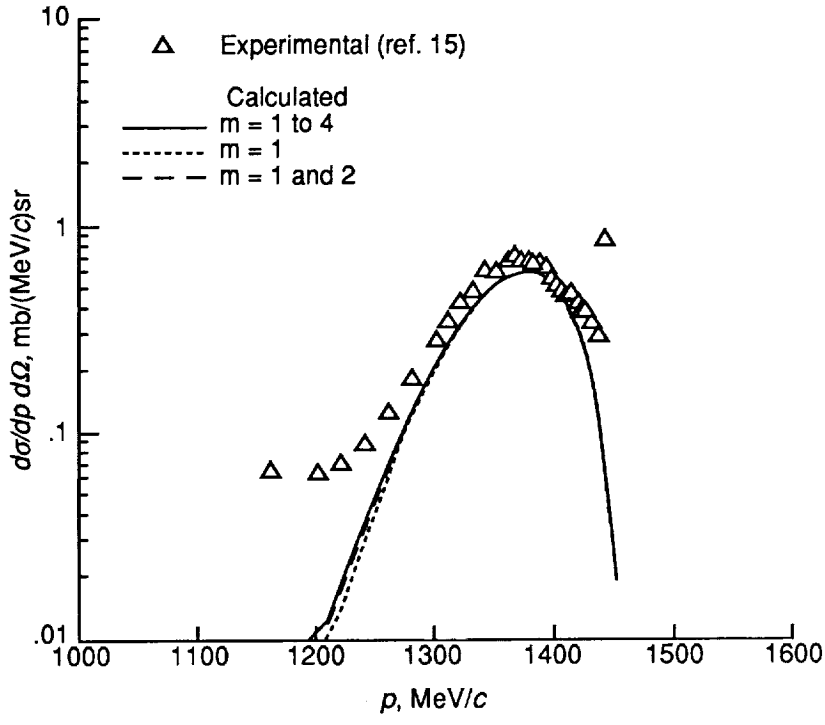

Figure 2. Inclusive proton scattering on ^{7}Li at 800 MeV for scattering angle of 15°.

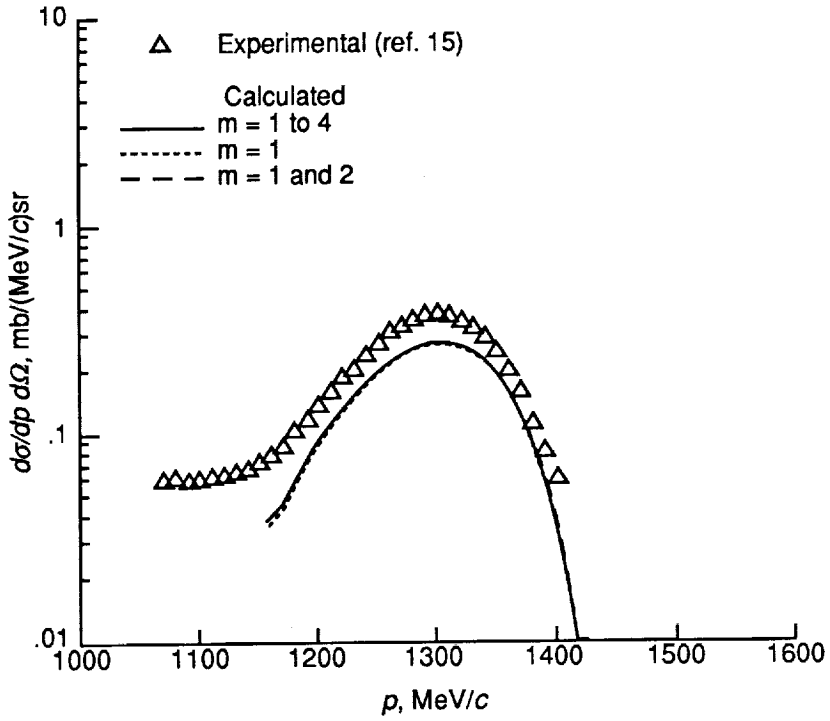

Figure 3. Inclusive proton scattering on ^{7}Li at 800 MeV for scattering angle of 20°.

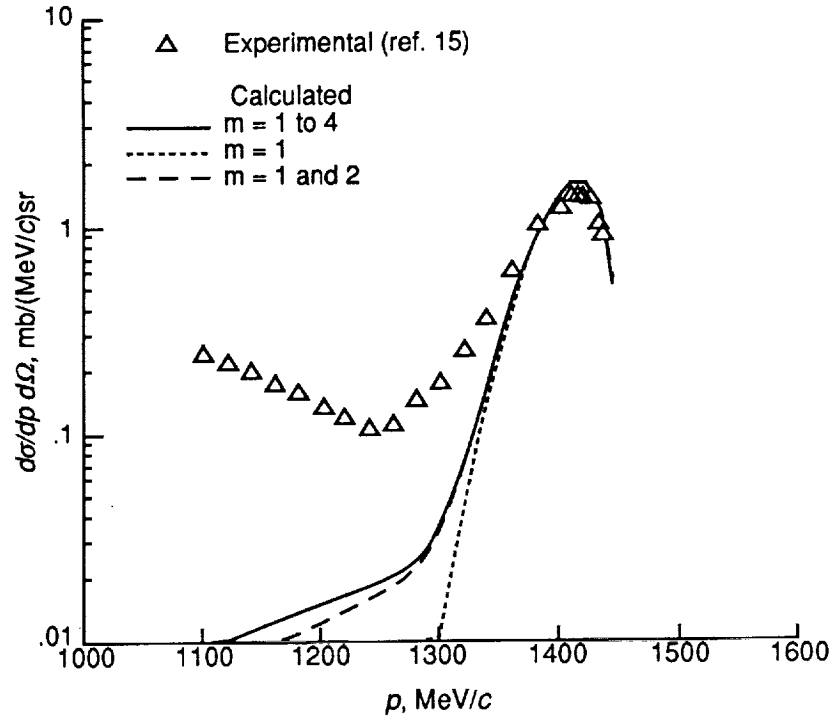

Figure 4. Inclusive inelastic proton scattering on ^{12}C at 800 MeV for scattering angle of 11°.

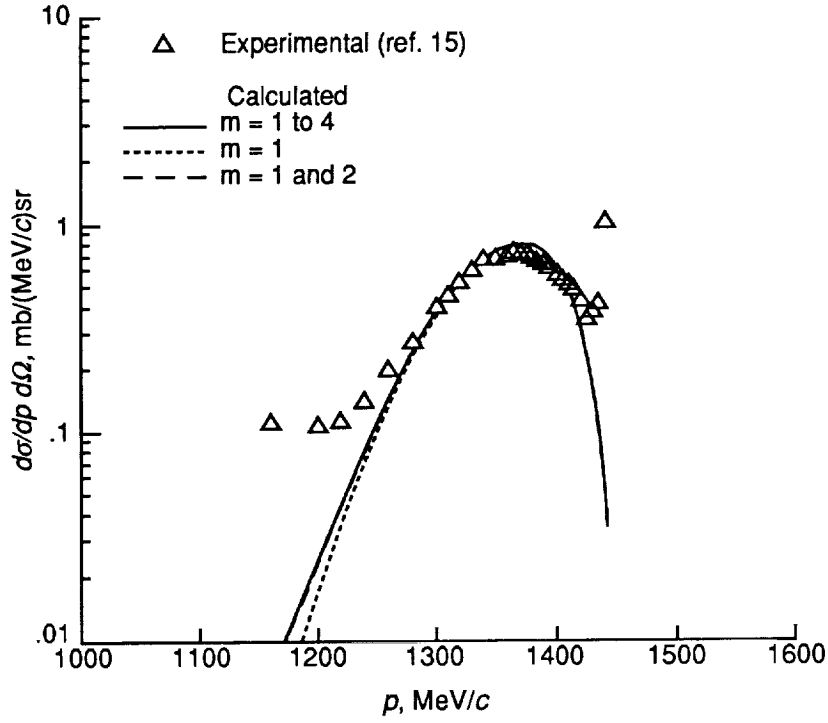

Figure 5. Inclusive inelastic proton scattering on ^{12}C at 800 MeV for scattering angle of 15°.

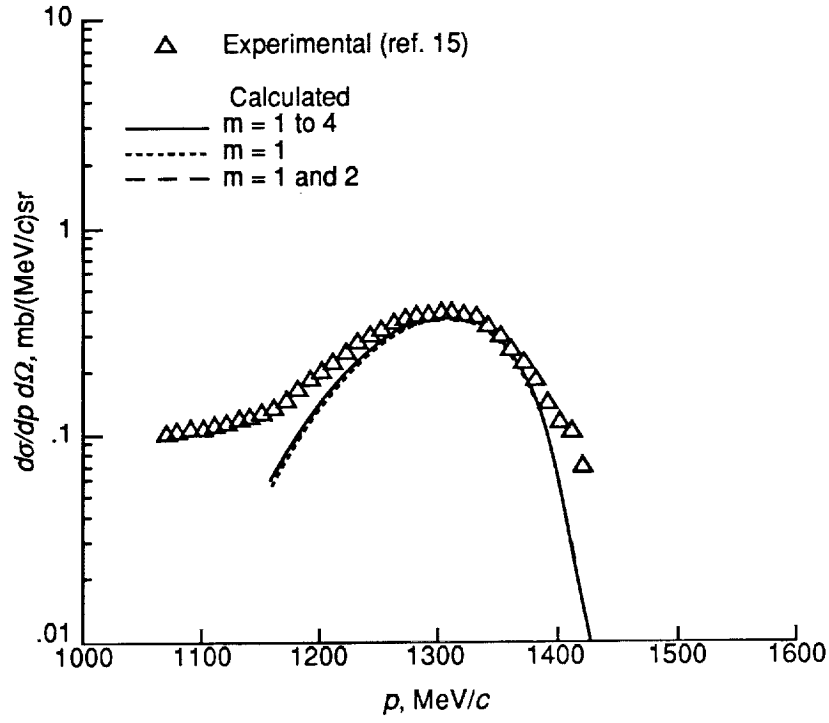

Figure 6. Inclusive inelastic proton scattering on ^{12}C at 800 MeV for scattering angle of 20°.

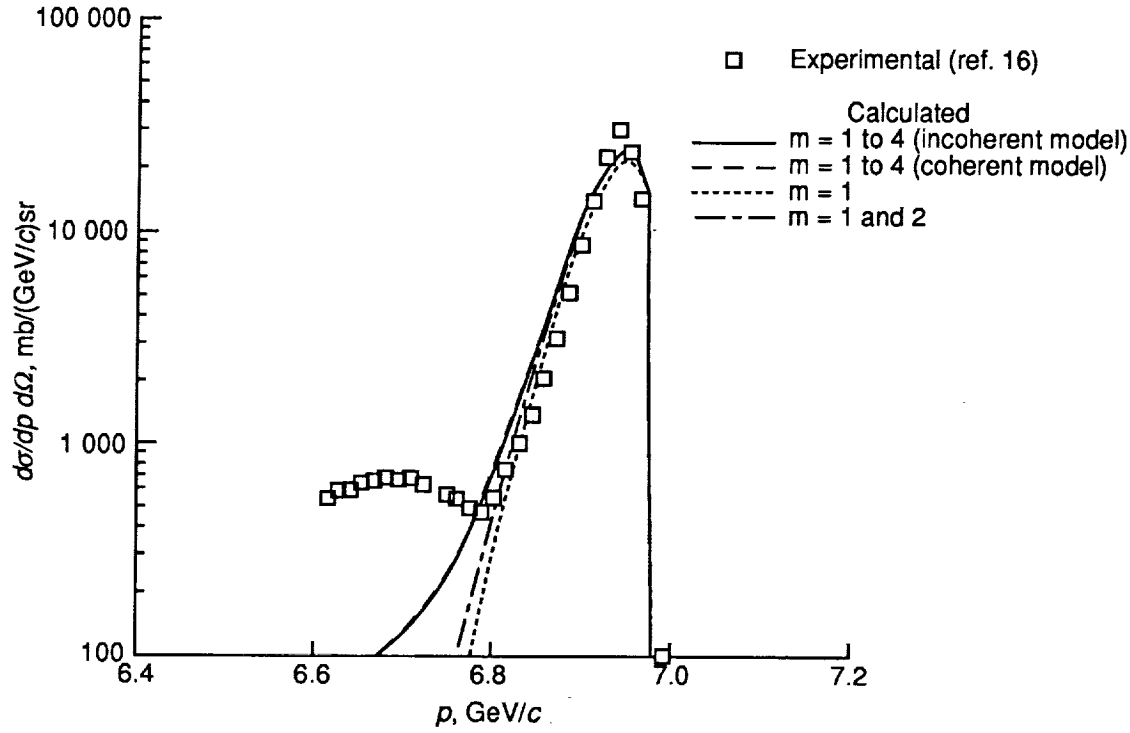

Figure 7. Inclusive ^{4}He scattering on ^{4}He at 1.05 GeV/amu for scattering angle of 2.112°.

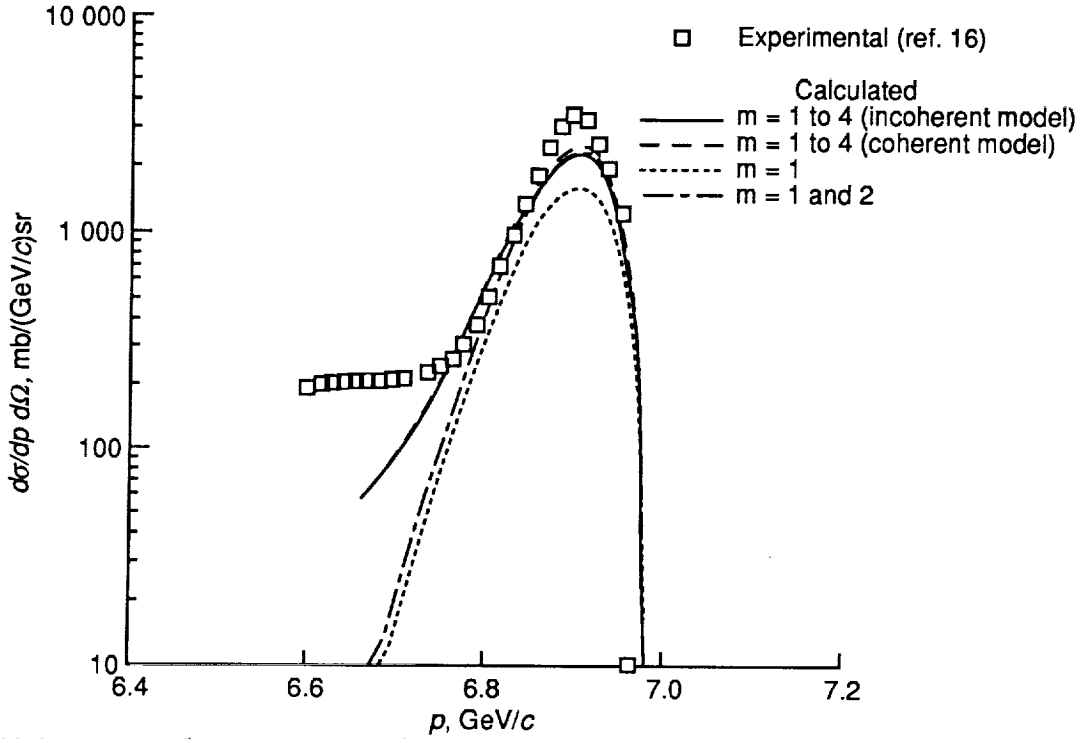

Figure 8. Inclusive ^{4}He scattering on ^{4}He at 1.05 GeV/amu for scattering angle of 3.094°.

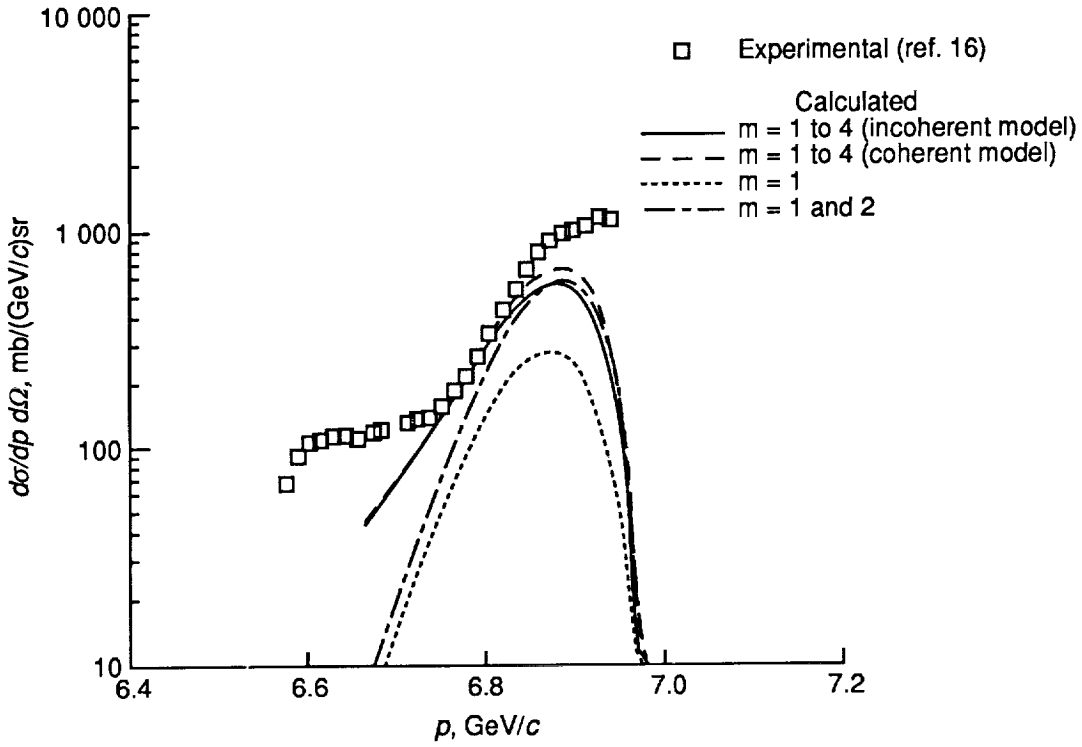

Figure 9. Inclusive ^{4}He scattering on ^{4}He at 1.05 GeV/amu for scattering angle of 3.630°.

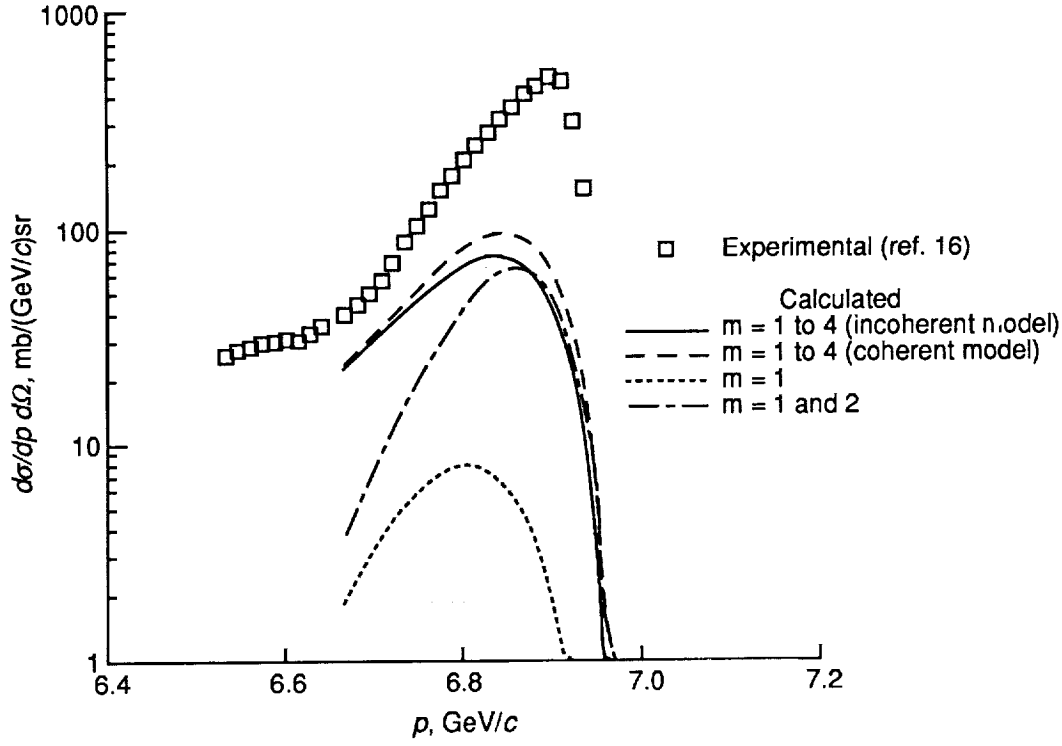

Figure 10. Inclusive ^{4}He scattering on ^{4}He at 1.05 GeV/amu for scattering angle of 4.552°.

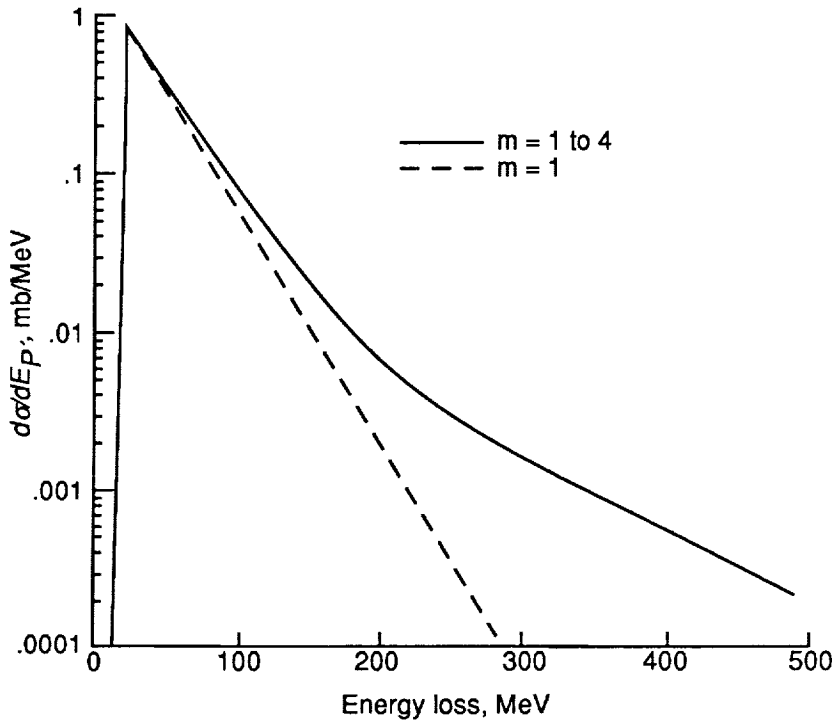

Figure 11. Energy loss spectrum for ^{4}He-^{4}He scattering at 1.05 GeV/amu.

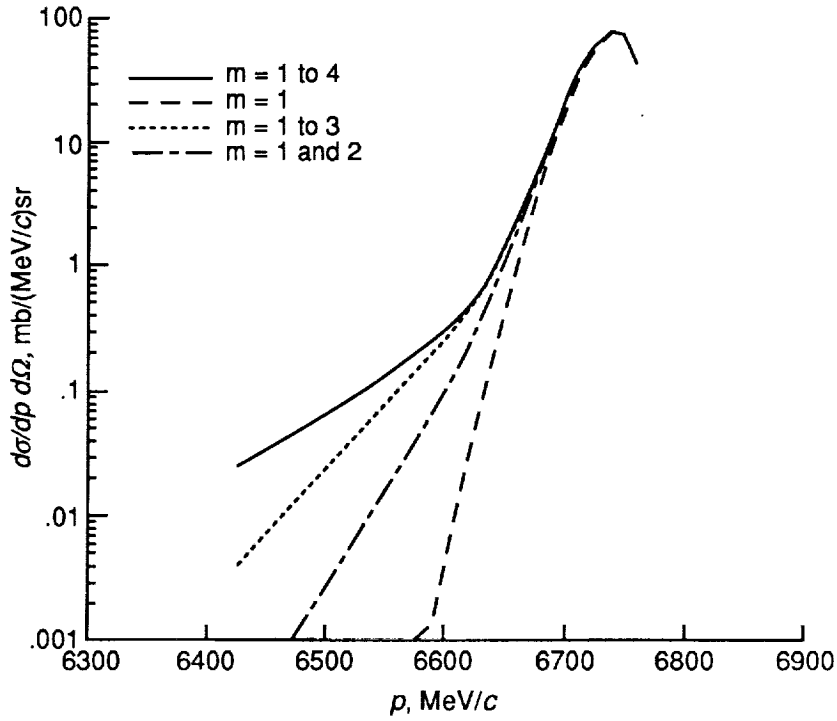

Figure 12. Inclusive ^{4}He scattering on ^{16}O at 1 GeV/amu for scattering angle of 1°.

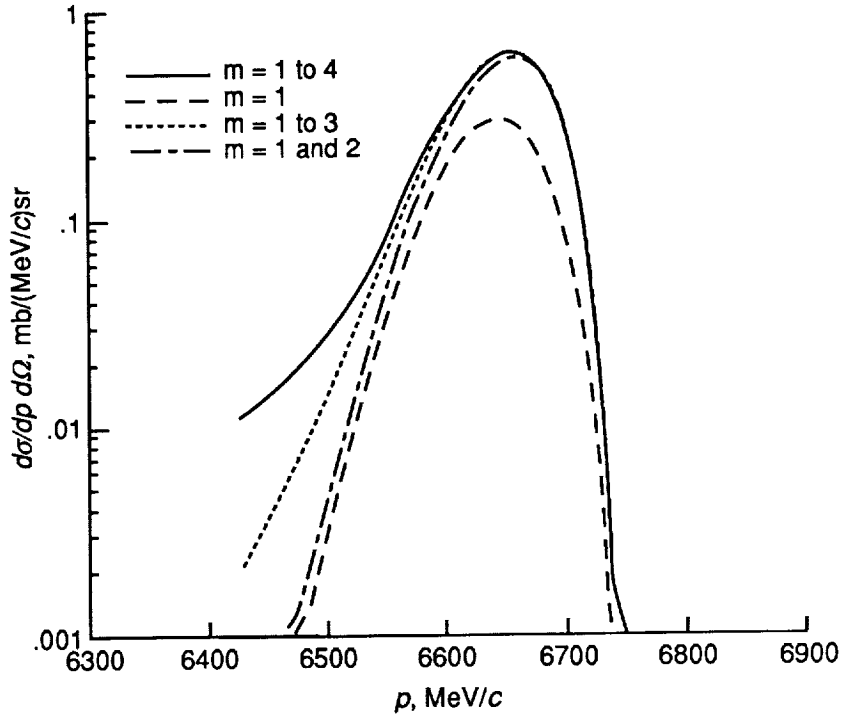

Figure 13. Inclusive ^{4}He scattering on ^{16}O at 1 GeV/amu for scattering angle of 4°.

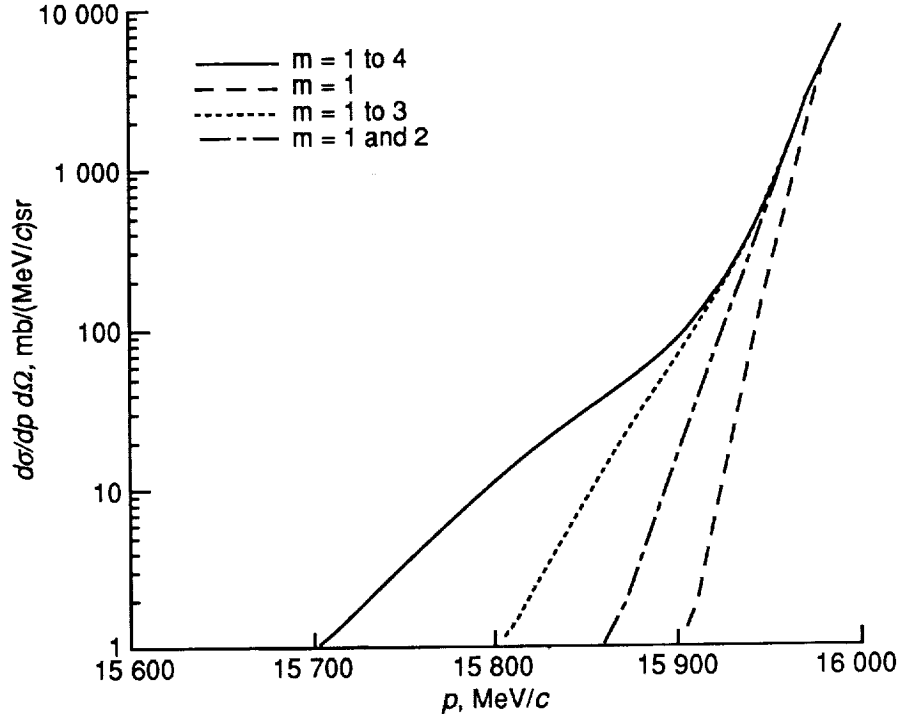

Figure 14. Inclusive ^{16}O scattering on ^{16}O at 1 GeV/amu for scattering angle of 0.5°.

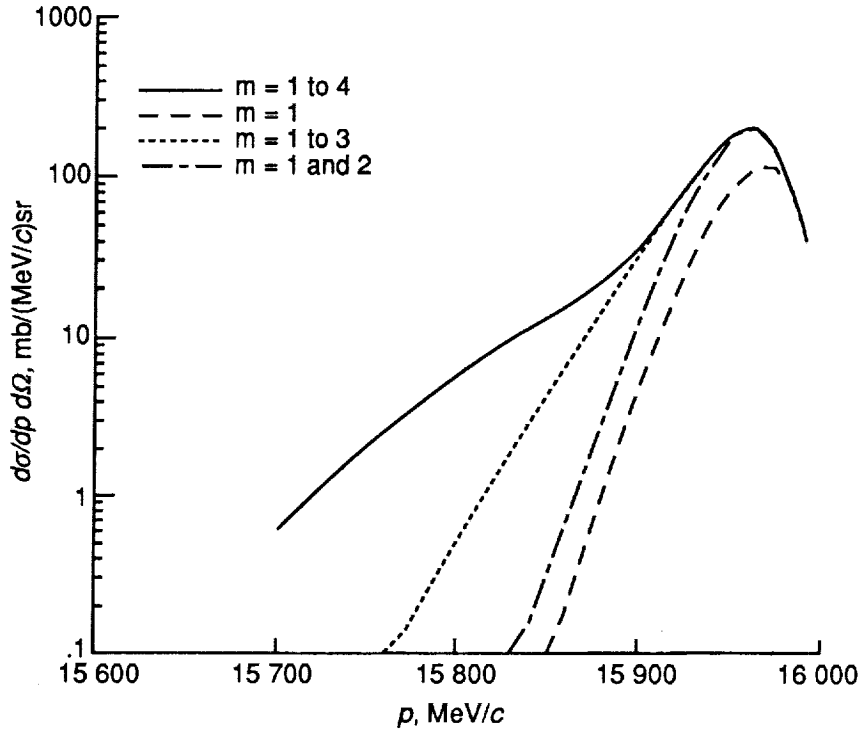

Figure 15. Inclusive ^{16}O scattering on ^{16}O at 1 GeV/amu for scattering angle of 1°.

REPORT DOCUMENTATION PAGE

Form Approved
OMB No. 0704-0188

1. AGENCY USE ONLY *(Leave blank)*	2. REPORT DATE	3. REPORT TYPE AND DATES COVERED
	May 1992	Technical Memorandum

4. TITLE AND SUBTITLE
Quasi-Elastic Nuclear Scattering at High Energies

5. FUNDING NUMBERS
WU 593-42-21-01

6. AUTHOR(S)
Francis A. Cucinotta, Lawrence W. Townsend, and John W. Wilson

7. PERFORMING ORGANIZATION NAME(S) AND ADDRESS(ES)
NASA Langley Research Center
Hampton, VA 23665-5225

8. PERFORMING ORGANIZATION REPORT NUMBER
L-17036

9. SPONSORING/MONITORING AGENCY NAME(S) AND ADDRESS(ES)
National Aeronautics and Space Administration
Washington, DC 20546-0001

10. SPONSORING/MONITORING AGENCY REPORT NUMBER
NASA TM-4362

11. SUPPLEMENTARY NOTES

12a. DISTRIBUTION/AVAILABILITY STATEMENT
Unclassified–Unlimited

Subject Category 73

12b. DISTRIBUTION CODE

13. ABSTRACT *(Maximum 200 words)*
The quasi-elastic scattering of two nuclei is considered in the high-energy optical model. Energy loss and momentum transfer spectra for projectile ions are evaluated in terms of an inelastic multiple-scattering series corresponding to multiple knockout of target nucleons. The leading-order correction to the coherent projectile approximation is evaluated. Calculations are compared with experiments.

14. SUBJECT TERMS
Nuclear reactions; Optical model; Inclusive reactions; Response functions

15. NUMBER OF PAGES
21

16. PRICE CODE
A03

17. SECURITY CLASSIFICATION OF REPORT	18. SECURITY CLASSIFICATION OF THIS PAGE	19. SECURITY CLASSIFICATION OF ABSTRACT	20. LIMITATION OF ABSTRACT
Unclassified	Unclassified		

NSN 7540-01-280-5500

Standard Form 298(Rev. 2-89)
Prescribed by ANSI Std. Z39-18
298-102

NASA-Langley, 1992